16th World Conference on Earthquake, 16WCEE 2017

Santiago Chile, January 9th to 13th 2017

Paper N° 3557 (Abstract ID)

Registration Code: S-Y1463693225

SYSTEM IDENTIFICATION AND MODELING OF AN 18-STORY BUILDING IN NEPAL USING POST-EARTHQUAKE AMBIENT VIBRATION DATA

H. Yu[1], A. Levine[2], M. Mohammed[3], T. van Oss[4], B. Moaveni[5], A.R. Barbosa[6], A. Stavridis[7]

[(1)] *Graduate Student, Dept. of Civil and Environmental Engineering, Tufts University, hanshun.yu@tufts.edu*
[(2)] *Undergraduate Student, Dept. of Civil and Environmental Engineering, Tufts University, annie.levine@tufts.edu*
[(3)] *Graduate Student, School of Civil and Construction Engineering. Oregon State University, mohammem@oregonstate.edu*
[(4)] *Graduate Student, Dept. of Civil, Structural and Environmental Engineering, University at Buffalo, tjvanoss@buffalo.edu*
[(5)] *Associate Professor, Dept. of Civil and Environmental Engineering, Tufts University, babak.moaveni@tufts.edu*
[(6)] *Assistant Professor, School of Civil and Construction Engineering. Oregon State University, andre.barbosa@oregonstate.edu*
[(7)] *Assistant Professor, Dept. of Civil, Structural and Environmental Engineering, University at Buffalo, astavrid@buffalo.edu*

Abstract

Investigating structures damaged by strong earthquakes can provide valuable insight in understanding the performance of structures during such events. Few studies have been conducted on structures using post-earthquake vibration data to assess their state of health/performance. This paper presents such a study by considering an 18-story apartment building damaged during the 7.8 Gorkha Earthquake that occurred in Nepal in April 25, 2015. The building was instrumented with 15 accelerometers in two configurations that measured its ambient vibration response. The recorded data is analyzed and the modal parameters of the test structure are identified using the Natural Excitation Technique combined with Eigensystem Realization Algorithm (NExT-ERA), an output-only system identification method. Moreover, a newly developed simplified analytical tool is used to simulate the response of the structure. This tool allows the estimation of the base shear-vs.-displacement curve for the structure in two orthogonal dimensions. A linear finite element (FE) model of the building was also developed. Masonry infill wall panels are modeled using the equivalent diagonal strut method approach. The building FE model is based on the geometry of the building and its material properties to estimate numerically the dynamic characteristics of the test structure. The identified modal parameters are compared to those obtained from the FE model to identify possible shortcomings of the identification and modeling approaches. It is observed that the identified natural frequency and mode shape of the first vibration mode are in reasonable agreement with the one obtained from the FE model. However, no such agreement is observed for the higher modes.

Keywords: 2015 Gorkha Nepal Earthquake; Post-earthquake performance assessment; System identification;

1. Introduction

Accurate assessment of the performance and the state of health of structures is an important and challenging task for structural engineers, especially with the increasing concerns about aging infrastructure and frequent natural disasters. Vibration-based structural health monitoring methods have been applied with reasonable success for characterizing the dynamic performance of different types of structures [1, 2]. These methods often rely on estimation of dynamic properties of structures from vibration measurements. System identification refers to the process of estimating the dynamic properties, such as the natural frequencies, mode shapes, and damping ratios of a structural system from its measured data. Small-scale simplified laboratory models have been successfully tested and analyzed using different methods; however, few large-scale or in-situ tests have been conducted on structures with varying levels of damage [3-6]. Reconciling the differences between control tests and real structures will help to calibrate and validate current numerical models for more precise response predictions. With increasing knowledge about building responses and dynamic properties, it can become possible to more accurately assess the structural performance and state of health, and provide the necessary preventative measures.

The magnitude 7.8 earthquake struck Nepal on April 25, 2015. According to the USGS, hundreds of aftershocks have occurred east of the main shock since (see Fig. 1). The main shock occurred around 80 km Northwest of Kathmandu, with sizable aftershock of 7.3 magnitude occurring on May 12 around 80 km Northeast of Kathmandu. A shake map from the USGS shows "broad, very strong shaking, elongated eastward from hypocenter by EQ finiteness [7]. More information on the performance of structures during the 2015 Gorkha Earthquake can be found in Brando et al. [8].

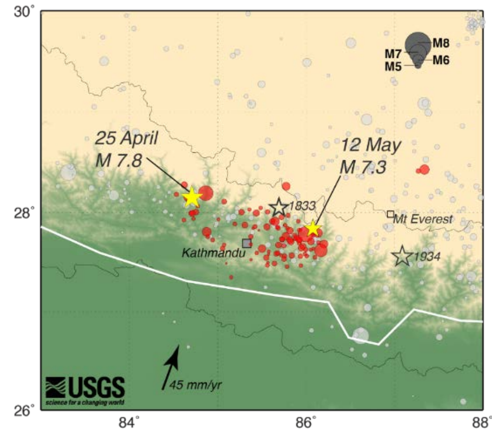

Fig. 1 – Aftershock map in Nepal [7]

This paper describes the system identification performed on a building that was damaged by the recent Gorkha earthquake and compares the data with a corresponding linear finite element (FE) model. The system identification used in this study is the Natural Excitation Technique combined with the Eigensystem Realization Algorithm (NExT-ERA) [9, 10]. In this method, vibration data is used to estimate a linear state-space model of a structure. The modal parameters, consisting of natural frequencies, damping ratios, and mode shapes, are extracted from the state-space model.

A linear finite element model of the undamaged stage of the structures is developed for this comparison. This model is somewhat useful for developing a general idea of the natural frequencies and mode shapes of the undamaged structure. However, the extensive level of damage observed in the infill walls, makes the development of a linear finite element for the damaged structure extremely complex, and this is left for follow-up studies. Comparison of the natural frequencies of the in-situ measured damaged structure with the ones from the model, clearly indicates that not all modal frequencies of the structure are identified, and other methods also need to be employed.

2. 18-Story Building and Instrumentation

2.1 Structural details

The structure is an 18-story (basement plus 17 stories above ground) high-rise reinforced concrete building as shown in Figure 2a. The floor plan is shown in Figure 2b. The location of the staircases and elevators can be seen to the right and left of the central lobby.

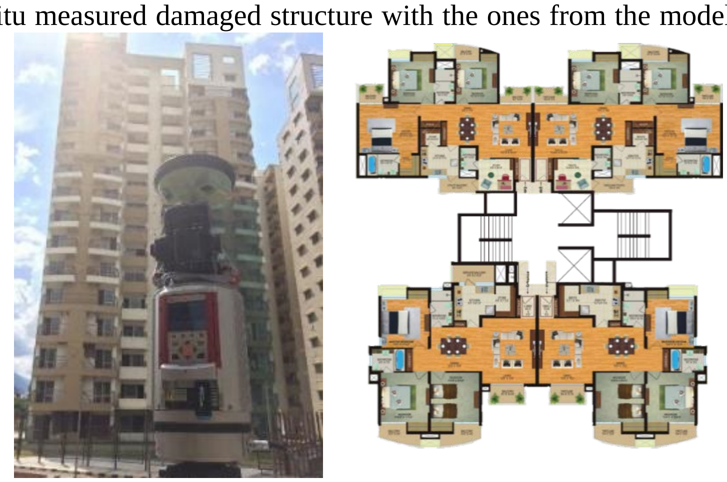

(a) (b)

Fig. 2 – 18-story building

2.2 Observed damage

Extensive non-structural and minor structural damage was observed in the building in the aftermath of the earthquake. Beam-column joint cracks and shear cracks were visible in coupling beams and short beams. Additionally, flexural cracks on beams propagated to the 6 inch slabs, especially in the coupling beams connecting the elevator cores. Figure 3 shows the observed damage at different components of the building. It is worth noting that even though the building suffered mainly non-structural damage, the building was not used for shelter in place, and at the time of the visit, it was expected that it may take up to 18-months for the building to be repaired and for people to be able to return to their homes.

Fig. 3 – Observed damaged in (a) corner of infill wall, (b) beam corner, c) exterior, d) interior/exterior wall

2.3 Instrumentation

The obtained data from the ambient vibration response of the building is used to identify the modal parameters. The vibration data were collected through 15 accelerometers that were installed in two distinct setups of sensor configurations: one setup on floors 9, 12, and 15, and the second setup on floors 3, 6 and 9. Fig. 4 shows the location of sensors on the 9th floor in both setups and the orientation for the north. On each floor, there were five to six accelerometers installed in: (1) the center of the building, (2) northwest corner, and (3) southeast corners of the building. The accelerometers measured acceleration in perpendicular horizontal directions. The data includes approximately 1.5 hours of ambient vibration recordings. The data from different setups were obtained over the same day. Table 1 provides the location and channel numbers of the sensors in Setup 1.

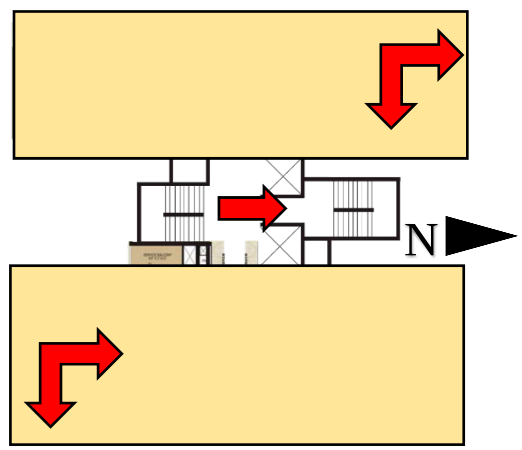

Fig. 4 – Sample sensor layout (floor 9)

The accelerometers were mounted on brackets that were then attached to various locations within the building using two-sided tape. The sensors were wired to a National Instruments compact DAQ through BNC cables and the data were saved on a laptop. Figure 5 shows the used compact DAQ and an in-situ sensor installation. The sensor calibration factors were updated post-data collection. A shaker (APS Electro-SEIS 420) was used to compute new calibration factors compared to a reference channel. The sensors were grouped together on the shaker in various configurations. Overall, the new calibration factors were found to be close to the original factors.

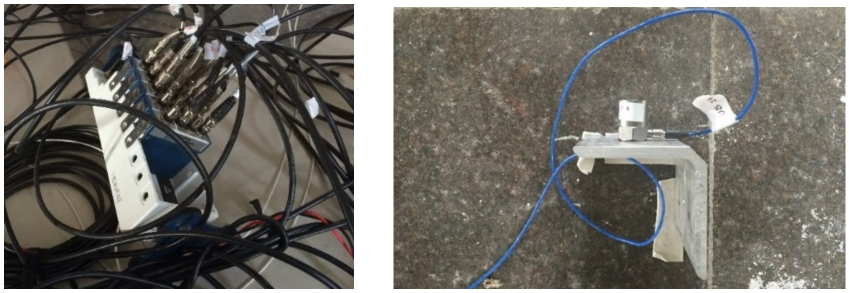

Fig. 5 – Sensor setup (a) DAQ system and (b) bracket mount

3. System Identification

3.1 Method

The NExT-ERA method [9, 10] is used to estimate the modal parameters of the building. According to the available data length in each setup, the recorded ambient vibration data is divided into 6 sets for each of Setups 1 and 2. Each data set is approximately corresponding to a 9- minute long ambient vibration except for the last dataset of Setup 1 that is approximately 6 minutes. All the data was cleaned by the following process: (1) applying a band-pass Finite Impulse Response (FIR) filter between 0.25 to 10 Hz, (2) down-sampling data from 2048 Hz to 256 Hz, and (3) removing voltage spikes in the time history. After inspecting the time history and power spectral density plots of all sensors, only measurements from sensors 1, 3, 4, 6, 9, 12, 14, and 15 from Setup 1 and sensors 1, 3, 4, 6, 8, 12, 14, and 15 from Setup 2 are considered in system identification. Noisy data from the other sensors could be due to the poor quality of BNC cables and/or their end connectors which were acquired locally in Nepal in the immediate aftermath of the earthquake and were connected on site under the one day time constraint that the research team had access to the site. Figure 6 shows the acceleration time history of cleaned data for the first dataset in Setup 1. Figure 7 plots the Fourier Amplitude Spectra (FAS) of the same dataset. The FAS plots provide distinct peaks in the ambient response of the building which correspond to the vibration modes.

Table 1 – Sensor layout for Setup 1

Sensor No.	Floor	Corner	Dir.	Channel No.
1	9	SE	N	1
2	9	SE	E	removed
3	12	SE	N	2
4	12	SE	E	3
5	9	M	N	removed
6	9	NW	N	4
7	9	NW	E	removed
8	15	SE	S	removed
9	15	SE	E	5
10	15	M	N	removed
11	15	NW	W	removed
12	15	NW	S	6
13	12	NW	N	removed
14	12	M	N	7
15	12	M	E	8

In the application of NExT, the cross power spectral densities of the considered channels are computed with two reference channels using 8 Hamming windows with 50% overlap. Two reference channels are chosen such that they are not located close to any modal node for vibration modes of interest. For Setup 1, reference channels are SE-N and SE-E on the 9th floor. For Setup 2 they are SE-N on the 9th floor and SE-E on the 6th floor. The free vibration data were estimated as inverse Fourier transformation of cross-power spectral densities, which was then fed to the ERA method. In the application of ERA, a Hankel matrix of size 3200×800 was formed based on 800 data points or 3.125 seconds of estimated free vibration data. Order of the state-space model to fit the data was selected using a stabilization diagram. Modal parameters were estimated from the eigenvalues and eigenvectors of the realized state-space systems for all the 12 data sets.

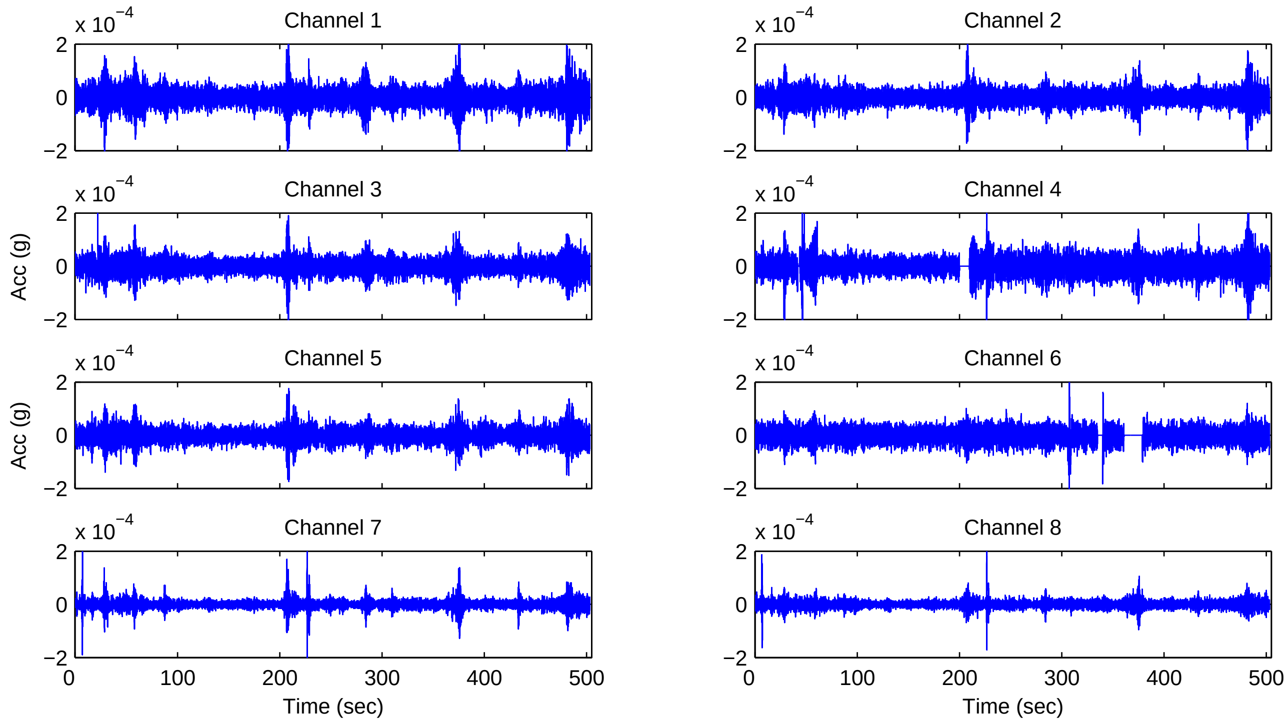

Fig.6 – Sample acceleration time history (dataset 1 Setup 1)

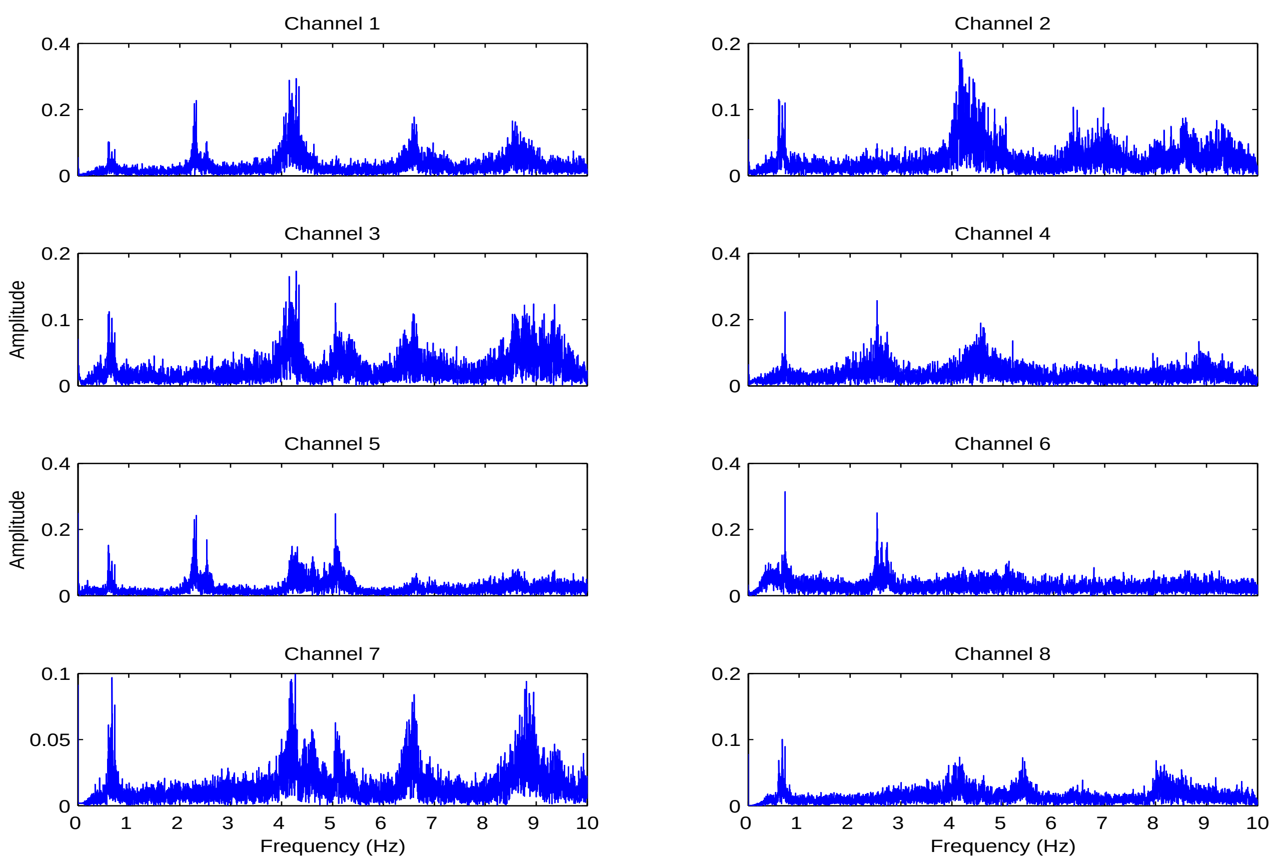

Fig.7 – Sample Fourier Amplitude Spectra (dataset 1 Setup 1)

3.2 Results

Figure 8 shows a sample stabilization diagram for Setup 1 and dataset 1. In this plot the identified natural frequencies are shown versus different model orders. The natural frequencies that are repeatedly identified at increasing orders are considered to be "stable." Vertical red lines indicate the stable modes of interest in this study.

Table 2 presents the statistics (mean and standard deviation over 6 datasets) of identified natural frequencies and damping ratios for each of the two setups. It can be seen that the natural frequencies are identified very consistently with very small standard deviations while the damping estimates show larger variability within each setup. Comparing the mean values of natural frequencies for the two setups, there is also an excellent agreement between the two setups with a maximum error of 2.3% (mode 3). So even for the ambient measurements with relatively low signal-to-noise-ratios, the natural frequencies of the lower modes are accurately and consistently identified. For the damping ratios, the mean values from the two setups are slightly different. The damping ratios show larger estimation uncertainty but they are still reasonable with the exception of the first mode. The damping ratio for the first mode is identified as 5.1% for Setup 1 and 7.5% for Setup 2 which are very large for a tall building. This can be due to the fact that there are three spectral peaks around the first modal frequency and the identification method tries to fit all of them with one mode resulting in inflated damping estimates.

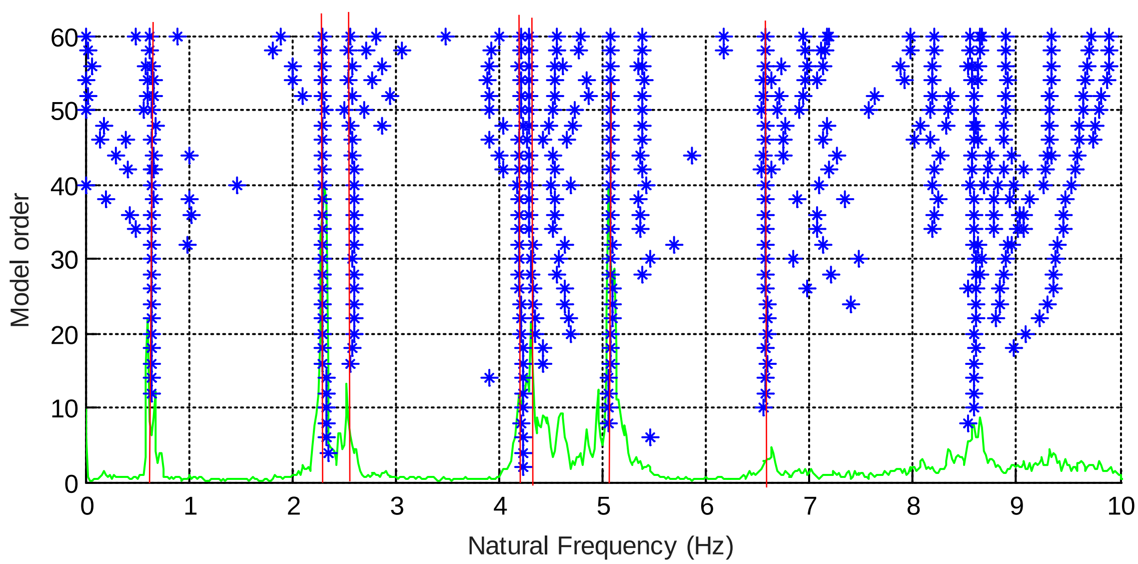

Fig.8 – Sample stabilization diagram

Table 2 – Statistics of the identified natural frequencies and damping ratios

Mode Number	Natural Frequencies [Hz] (mean, std)		Damping ratios [%] (mean, std)	
	Setup 1	Setup 2	Setup 1	Setup 2
1	0.62, 0.01	0.62, 0.02	5.1, 2.3	7.5, 1.2
2	2.30, 0.00	2.29, 0.00	2.1, 0.2	1.5, 0.1
3	2.60, 0.02	2.54, 0.02	1.3, 0.2	1.6, 0.2
4	4.20, 0.02	4.18, 0.01	2.2, 0.5	1.7, 0.5
5	4.30, 0.02	4.28, 0.01	0.9, 0.3	0.8, 0.2
6	5.08, 0.02	5.06, 0.03	1.3, 0.5	1.4, 0.6
7	6.58, 0.04	6.55, 0.01	1.2, 0.4	1.8, 0.9

Mode shapes are also estimated for each dataset and the two setups. An average mode shape is estimated for each setup based on the reliable mode shape estimates from the 6 datasets. To determine the "reliable mode shapes" to be used in the average, MAC values between different datasets are computed. Table 3 shows the MAC values between the mode shapes identified from dataset 2 and the other 5 datasets. The dataset with the MAC value lower than 0.9 were deemed unreliable and not used in averaging. Table 4 lists the datasets considered in the averaging process for Setups 1 and 2. Once average mode shapes of Setups 1 and 2 are obtained, these mode shapes are combined to represent the complete mode shapes of building along its full height. The shapes from the two setups are combined by normalizing the mode shapes to one of the two channels that are available for both setups: Channel 1 (SE-N on 9th floor) and Channel 4 (NW-N on 9th floor).

Table 3 –MAC values between mode shapes from dataset 2 and other datasets

	Reference dataset 2				
	Set1	Set3	Set4	Set5	Set6
Mode1	0.84	0.94	0.95	0.94	0.87
Mode2	0.98	0.99	0.99	0.99	0.97
Mode3	0.97	0.98	0.97	0.92	0.96
Mode4	0.97	0.97	0.95	0.97	0.97
Mode5	0.61	0.98	0.90	0.90	0.58
Mode6	0.96	0.89	0.98	0.95	0.97
Mode7	0.87	0.96	0.89	0.72	0.91

Table 4 – Datasets used in the average for Setups 1 and 2

	Mode 1	Mode 2	Mode 3	Mode 4	Mode 5	Mode 6	Mode 7
Setup 1	1, 3, 4, 5, 6	all	all	all	2, 3, 4, 5	all	1, 2, 3, 4, 6
Setup 2	1, 2, 3, 4, 6	all	all	all	2, 3, 5, 6	1, 2, 3, 4, 6	1, 2, 4, 5

MAC values between the two sets of mode shapes are shown in Table 5. The high MAC values for modes 1, 3, 4, 5, and 6 indicate that these modes are identified consistently using different references. The MAC values of modes 2, and 7 (0.80-0.85) indicate that there is some inconsistency between the two sets of identified results that can be due to estimation errors. Considering the modal contribution of each mode to Channels 1 and 4, the following reference channels are selected for modes 1-7, respectively: 1, 1, 1, 4, 4, 4, 1. Figure 9 plots the combined mode shapes using the selected reference channels while the complex values of mode shapes are plotted in Figure 10 as compass plots. In Figure 9, the mark '*' indicates the position of reference channel used for normalization while the mark '+' indicates the value of the other reference channel not used for normalization. From Figure 9 it can be seen that all of the identified modes have some torsional components. The complex mode shape components appear to be scattered in the complex plane indicating identification of non-proportional modes. The fact that all the modes are identified as non-proportional can also be a symptom of larger identification errors for the mode shapes.

Table 5 – MAC values between mode shapes with reference Channels 1 and 4

Mode1	Mode2	Mode3	Mode4	Mode5	Mode6	Mode7
0.94	0.85	0.93	0.97	1.00	0.96	0.80

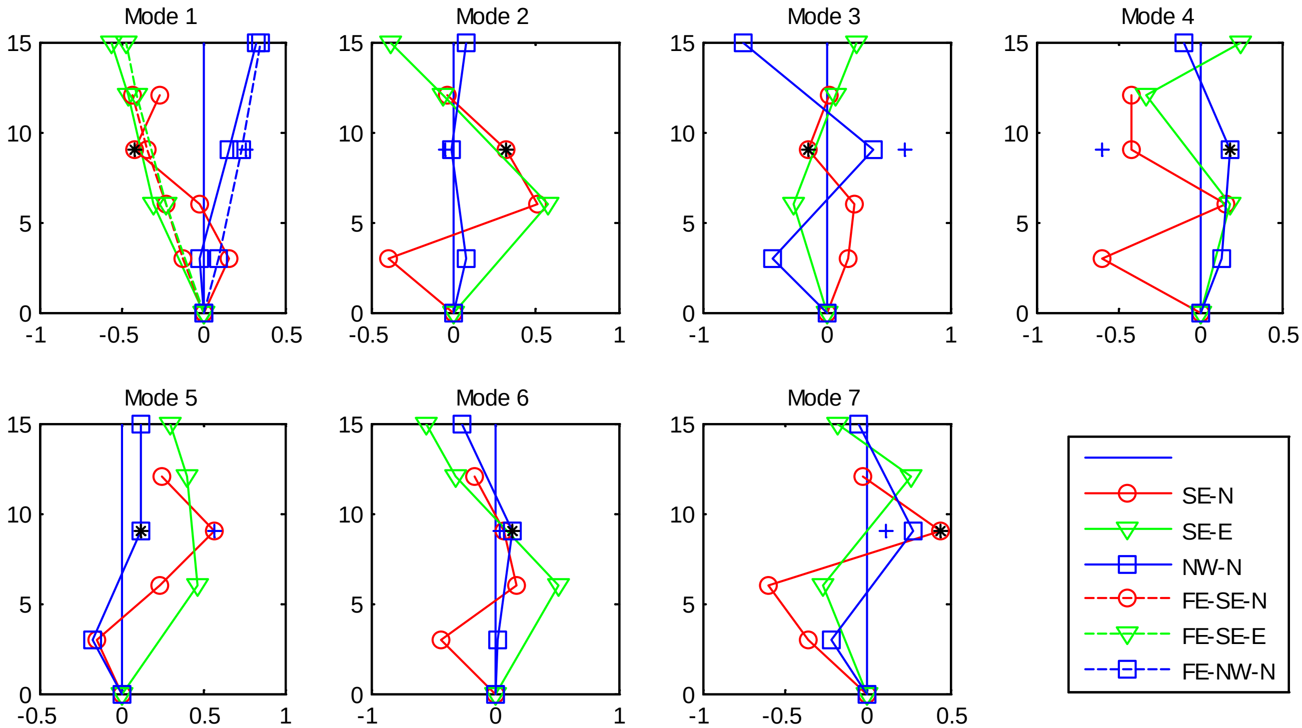

Fig. 9 – Identified mode shapes from both setups combined (together with mode shape 1 from FE model)

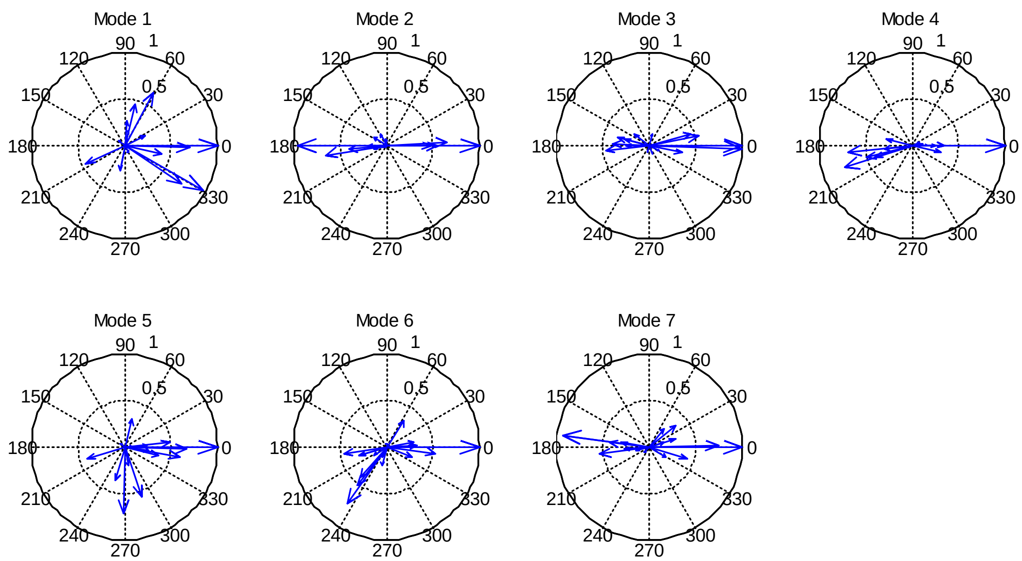

Fig. 10 – Compass plot of identified mode shape

4. Modeling

4.1. Simplified Model

A recently developed analytical tool is used to estimate the base shear-vs. first story drift curve of the structure [11]. The method estimates the force-vs.-displacement curves for each bay of the RC frame of first story of the building by defining a quadrilinear curve that has been found to estimate with sufficient accuracy the initial stiffness, apparent yield point, peak strength, the peak and residual strengths, as well as the drifts associated with these points. The method has been applied to all bare and infilled frames, including the infills with openings whose stiffness and strength have been adjusted accordingly [12]. The method has not considered the masonry walls that are not confined with columns on both sides. Such walls are common in Nepal and are used to enclose the balcony areas in the perimeter. The inspection of the structure indicated that these walls were severely damaged along the height of the structure, and hence it is unknown if they contributed meaningfully to the lateral resistance.

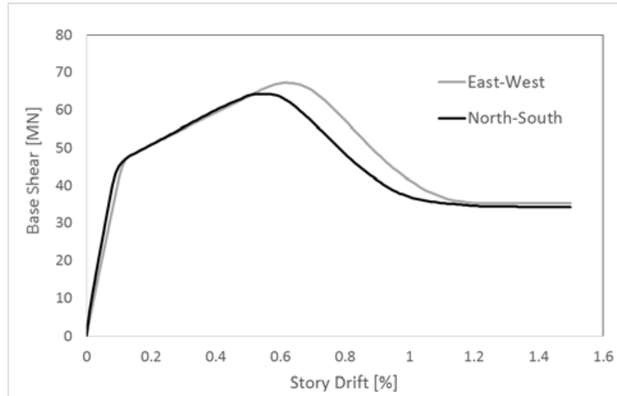

Fig. 11 – Estimated base shear-vs.-first story drift

4.2. FE Model

The Sap2000 software [13] is used to develop a linear model for the 18-story building with the infill walls (Figure 12). The typical story height is 3.0 m. All RC beams are assumed to have a 500 mm × 350 mm cross sectional dimensions. RC column dimensions were obtained from the design drawings. The slabs are 125 mm thick. For the RC elements (beams, columns and shear walls) in this model, a compressive strength of 25 MPa is used to define the mechanical properties of the RC members, using ACI 318 equations. The RC columns and RC beams are modeled using linear elastic beam-column elements ($EI_{columns} = 0.7\ EI_{gross}$; $EI_{beams} = 0.3\ EI_{gross}$). The shear walls are modeled using linear elastic shell elements (no reduction flexural reduction factor was considered). To model the infill walls, the equivalent diagonal strut method is used. In this method, each infill wall is replaced with two compression only diagonal struts. Two types of infill walls are considered: (1) 240 mm thick exterior walls, and (2) 120 mm thick interior walls. The guidelines in FEMA 356-2000 [14], which are based on Stafford-Smith and Carter [15] and Mainstone [16], are used to determine the equivalent width of the struts. For the FEMA equations, it is assumed that the masonry compressive strength is 4.5 MPa and the elastic modulus equals to 2400 MPa. Stiffness reduction factors are applied to account for openings depending on size and location as per design drawings. Values of the stiffness reduction factors range from 0.3 to 0.7.

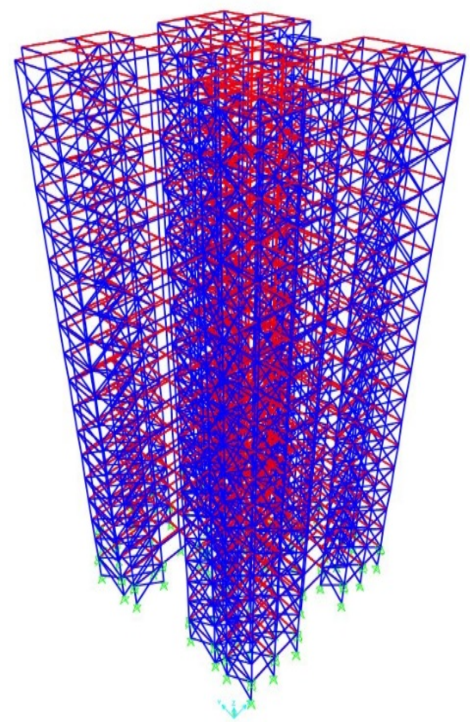

Fig. 12 – FE model

As in the analytical method described in the previous section, in this model, only the walls with columns at both ends of the infill panel are included as the walls with only one column at one end of the infill panel are not modeled. This modeling approach needs to be further validated with numerical analyses using applied element method that are currently under way. Linear modal analysis was performed to obtain the natural frequencies, periods and mode shapes of the building. Table 6 shows the natural frequencies and periods of the model. Figure 13 shows the obtained mode shapes of the model. For first mode, the FE model results are comparable to that of system identification (see Figure 9). The natural frequency from system identification is 0.62 Hz while that from the FE model is 0.55 Hz. The Modal Assurance Criterion (MAC) value between the identified first mode shape and that from the FE model is 0.82. The first mode shape of the FE model is also plotted on Figure 9 for comparison. It is also worth noting that the MAC value for the first mode shape increases to 0.95 if the SE-N data is ignored.

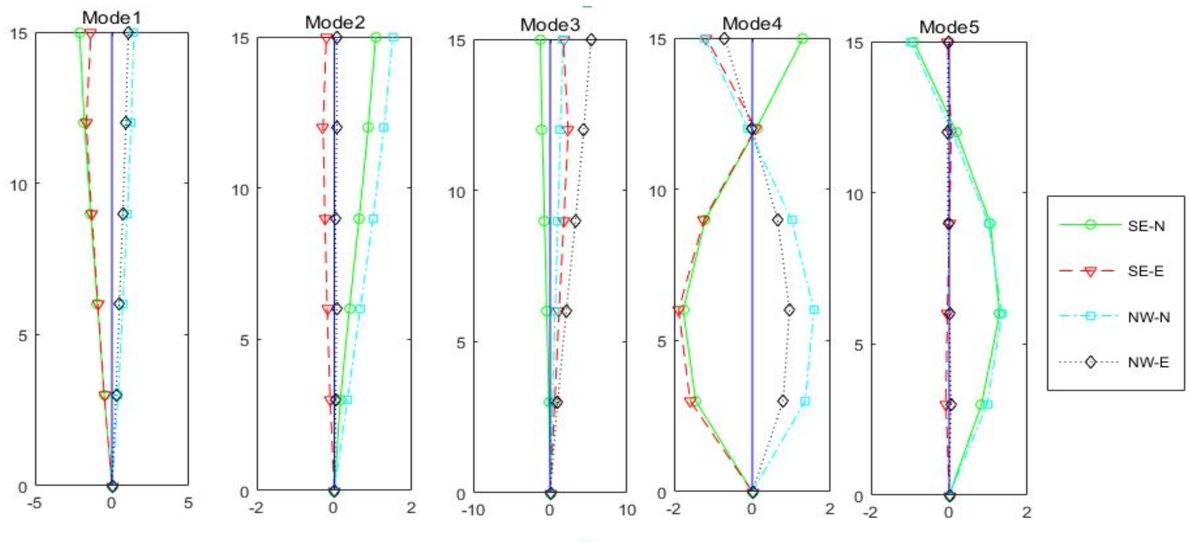

Fig. 13– Mode shapes of the model

Table 6 – Summary of natural frequencies and mass participation factors of the model

	Mode1	Mode2	Mode3	Mode4	Mode5
Frequency [Hz]	0.55	0.62	0.74	1.69	2.01
Cumulative Contribution in N-S	0.021	0.733	0.735	0.736	0.872
Cumulative Contribution in E-W	0.057	0.065	0.739	0.750	0.751
Cumulative Contribution in Torsion	0.703	0.724	0.779	0.901	0.901

5. Conclusions

This paper investigates the dynamic performance of an 18-story building in Nepal which was damaged during the 2015 Gorkha earthquake. The modal parameters of the building are extracted using the measured ambient vibration measurements. The natural frequencies are accurately and consistently identified using different subsets of data. The damping ratios are also estimated with reasonable accuracy. However, the first mode damping estimate appear to be too large for a tall building which can be inflated by the low identification order. In future works, higher model orders and other identification methods should be tested. A linear FE model of the building is also created based on the geometry and material properties. For the natural frequency and mode shape of the first vibration mode, there is reasonable consistency between the FE model and identification results. However, there is not a good correlation between the model and data for the higher modes.

6. Acknowledgements

Partial support of this study by the National Science Foundation Grants 1545632, 1545595, and 1254338 is gratefully acknowledged. The authors express their gratitude to Mr. Supratik Bose, Mr. Rajendra Soti, Mr. Patrick Burns, and Dr. Richard Wood for their assistance in the collection of data. The opinions, findings, and conclusions expressed in this paper are those of the authors and do not necessarily represent the views of the organizations and collaborators involved in this project.

7. References

[1] Sohn H, Farrar CR, Hemez FM, Shunk DD, Stinemates DW, Nadler BR et al (2004): *A review of structural health monitoring literature*: 1996-2001: Los Alamos National Laboratory Los Alamos, NM.

[2] Carden EP, Fanning P (2004): Vibration based condition monitoring: A review. *Structural Health Monitoring*, **3** (4), 355-377.

[3] Huth O, Feltrin G, Maeck J, Kilic N, Motavalli M (2005): Damage identification using modal data: Experiences on a prestressed concrete bridge. *Journal of Structural Engineering*, **131** (12), 1898-1910.

[4] Reynders E, Roeck GD, Gundes Bakir P, Sauvage C (2007): Damage identification on the Tilff bridge by vibration monitoring using optical fiber strain sensors. *Journal of Engineering Mechanics*, **133** (2), 185-193.

[5] Behmanesh I, Moaveni B. (2015): Probabilistic identification of simulated damage on the Dowling Hall Footbridge through Bayesian FE model updating. *Structural Control and Health Monitoring*, **22** (3), 463-483.

[6] Belleri A, Moaveni B, Restrepo JI (2014): Damage assessment through structural identification of a large-scale three-story precast concrete structure. *Earthquake Engineering and Structural Dynamics*, **43** (1), 61-76.

[7] Briggs R, Jaiswal K, McNamara D, Wald D, Benz H, Hearn M, Earle P (2015): The April-May 2015 Nepal Earthquake Sequence. *Earthquake Educational Slides, U.S. Geological Survey, National Earthquake Information Center. http://earthquake.usgs.gov/learn/topics/Nepal_Slides.pdf*

[8] Brando G, Rapone D, Spacone E, Barbosa A, Olsen M, Gillins D, Soti R, Varum H, Arede A, Vila-Pouca N, Furtado A, Oliveira J, Rodrigues H, Stavridis A, Bose S, Fagella M, Gigliotti R, Wood R (2015): Reconnaissance report on the 2015 Gorkha Earthquake effects in Nepal. *XVI Convegno Anidis*, L'Aquila, Italy.

[9] James GH, Carne TG, Lauffer JP (1993): The Natural Excitation Technique for modal parameters extraction from operating wind turbines. *Technical Report, Sandia National Laboratories*, SAND92-1666, UC-261, Sandia, New Mexico, USA.

[10] Juang JN, Pappa RS (1985): An eigensystem realization algorithm for model parameter identification and model reduction. *Journal of Guidance Control Dynamics*; **8** (5), 620-627

[11] Reese A, Stavridis A (2014): A simplified method for the estimation of the seismic resistance of RC frames with weak infill panels. *10th National Conference on Earthquake Engineering*, Anchorage, Alaska.

[12] Stavridis, A (2009): Analytical and Experimental Study of Seismic Performance of Reinforced Concrete Frames Infilled with Masonry Walls, Ph.D. Dissertation, University of California at San Diego, La Jolla CA.

[13] Computers and Structures Inc., *SAP2000 V.16 software*, 2013.

[14] FEMA (2000). FEMA-356, Prestandard and commentary for the seismic rehabilitation of buildings. Federal Emergency Management Agency, Washington, D.C., USA.

[15] Stafford SB and Carter, C (1969): A Method for the Analysis of Infilled Frames. *Proceedings of the Institution of Civil Engineers*, **44** (1), 31-48.

[16] Mainstone, R. (1971): On the Stiffnesses and Strengths of Infilled Frames. *Proceedings of the Institution of Civil Engineers*, Supplement IV, 57-90.